Radiology: Cardiothoracic Imaging

ORIGINAL RESEARCH

4D Flow Vorticity Visualization Predicts Regions of Quantitative Flow Inconsistency for Optimal Blood Flow Measurement

Francisco J. Contijoch, PhD • Michael Horowitz, MD, PhD • Evan Masutani, BS • Seth Kligerman, MD • Albert Hsiao, MD, PhD

From the Department of Bioengineering, Jacobs School of Engineering (F.J.C.) and Department of Radiology, School of Medicine (F.J.C., M.H., E.M., S.K., A.H.), UC San Diego, 9500 Gilman Dr, MC0412, La Jolla, CA 92093-0412. Received March 20, 2019; revision requested May 7; revision received September 3; accepted September 16. **Address correspondence to** F.C. (e-mail: *fcontijoch@ucsd.edu*).

Supported by the National Institutes of Health (grant NIH NHLBI K01 HL143113-01).

Conflicts of interest are listed at the end of this article.

See also the commentary by Markl in this issue.

Radiology: Cardiothoracic Imaging 2020; 2(1):e190054 • https://doi.org/10.1148/ryct.2020190054 • Content codes: CA MR

Purpose: To evaluate whether automated vorticity mapping four-dimensional (4D) flow MRI can identify regions of quantitative flow inconsistency.

Materials and Methods: In this retrospective study, 35 consecutive patients who underwent MR angiography with 4D flow MRI at 3.0 T from December 2017 to October 2018 were analyzed using a λ_2-based technique for vorticity visualization and quantification. The patients were aged 58.6 years ± 14.4 (standard deviation), 12 were women, 18 had ascending aortic aneurysms (maximal diameter > 4.0 cm), and 10 had bicuspid aortic valves. Flow measurements were made in the ascending aorta (aAo), mid-descending aorta, main pulmonary artery, and superior vena cava. Statistical tests included *t* tests and *F* tests with a type I error threshold (α) of .05.

Results: The 35 patients were visually classified as having no (n = 9), mild (n = 8), moderate (n = 11), or severe vorticity (n = 7). Across all patients, standard deviation of cardiac output in the aAo (0.58 L/min ± 0.45) was significantly (P < .001) higher than in the pulmonary arteries (0.15 L/min ± 0.10) and descending aorta and superior vena cava (0.14 L/min ± 0.12). The standard deviation of cardiac output observed in the aAo was significantly greater (P < .01) in patients with moderate or severe vorticity (0.73 L/min ± 0.55) than in those with none or mild vorticity (0.44 L/min ± 0.26).

Conclusion: Cardiac output and blood flow are essential MRI measurements in the evaluation of structural heart disease. Vorticity visualization may be used to help guide optimal location for flow quantification.

© RSNA, 2020

Phase-contrast MRI is the reference standard for noninvasive quantification of blood flow. Both planar phase-contrast and volumetric phase-contrast (four-dimensional [4D] flow) MRI are used to assess cardiovascular blood flow by integrating the through-plane component of velocity in a planar region of interest (ROI) (1) and have been validated in a variety of settings (2,3). 4D flow has recently become clinically viable with improvements in acquisition time associated with advances in parallel imaging and compressed sensing (4). One advantage of 4D flow is the ability to delineate any number of ROIs from a single volumetric acquisition. This enables retrospective interrogation of flow within multiple vessels or at multiple locations within a single vessel (5).

A natural question that arises in the analysis of 4D flow data is where measurements should be optimally performed. For example, flow measured anywhere along the ascending aorta (aAo) (between the sinotubular junction and origin of the brachiocephalic artery) should theoretically be identical via conservation of mass, as given by the continuity equation. However, inconsistency in flow measurements may arise owing to either imaging or anatomic artifacts. For example, a local signal void, owing to a stent or sternal wire, can distort the flow signal and prevent accurate flow measurement. When such an artifact is observed during interpretation, the measurement locations can be adjusted by drawing a different ROI (4D flow) at an alternate location.

However, it can be more difficult to observe and adjust for anatomic causes of flow inconsistency. Inconsistencies in the measured vector field may be due to complex flow patterns—namely, near a regurgitant valve, stenotic valve, or aneurysmal vessel (6)—and may lack apparent imaging artifacts and may limit the ability of the reader to perceive the underlying cause. Clinically, cardiovascular imagers can try to first identify these scenarios and then adjust measurement locations (7), but the spatial extent of the affected locations may be unclear. Vortical flow—one example of a complex flow pattern—is frequently observed in patients with ascending aortic aneurysms. We hypothesized that locations with flow inconsistencies might be more easily identified by visualizing regions of vortical flow, which may be computed directly from the velocity vector field.

Although identification and measurement of vortices in time-varying three-dimensional flow fields is an area of active fluid mechanics research and the field has

This copy is for personal use only. To order printed copies, contact reprints@rsna.org

Abbreviations

aAo = ascending aorta, dAo = descending aorta, 4D = four-dimensional, mPA = main pulmonary artery, ROI = region of interest, SVC = superior vena cava

Summary

Visualization of flow vorticity can highlight regions of flow inconsistency, which may help determine optimal locations for quantification of blood flow with four-dimensional flow MRI.

Key Points

- Flow vorticity can be visualized by using an automated pipeline without the need for vessel contouring or particle tracing.
- Increased ascending aorta (aAo) vortical flow is associated with greater error in blood flow measurements.
- Vorticity visualization may be used to avoid errors in flow quantification in error-prone regions such as the aAo in patients with aortic aneurysms.

yet to converge on a single definition or quantitative approach (8), several methods have been proposed for use in 4D flow (9). λ_2-based estimates (10) have been shown to provide reasonable approximations of vortical regions (11–13). In this study, we developed a segmentation-free approach to visualize regions of vorticity, analogous to a recently described wall shear stress technique (14). We evaluated whether vortical flow correlated with flow inconsistencies by measuring volumetric blood flow at multiple locations in the cardiovascular system. Furthermore, we compared variations in measured flow with a visual assessment of vortical flow regions. We specifically performed our analysis in a population of patients with ascending aortic aneurysms where we have frequently observed flow inconsistencies clinically.

Materials and Methods

Patient Demographics

With institutional review board approval and waiver of informed consent, we retrospectively evaluated 35 consecutive patients who underwent diagnostic quality MR angiography with 4D flow for the evaluation of a bicuspid aortic valve, suspected of having or known to have ascending aortic aneurysm between December 1, 2017, and October 1, 2018. The demographics of the patients are shown in Table 1. Maximal orthogonal biaxial aortic measurements were obtained from the 4D flow MR angiography. The presence of an ascending aortic aneurysm was defined as a maximal diameter exceeding 4.0 cm. Pediatric patients and patients with congenital heart disease other than a bicuspid aortic valve were excluded. Patients with intracardiac and extracardiac shunts were not included.

MRI Technique

4D flow was performed following the administration of intravenous gadolinium contrast material (gadobenate dimeglumine, 0.1 mmol/kg). We used a previously described cardiac-gated, four-point encoded variable-density pseudorandomly ordered Cartesian sequence followed by iterative compressed-sensing and parallel imaging reconstruction with respiratory self-navigation (4,15) with a 32-channel body receiver coil on a 3-T Discovery 750 (GE Healthcare, Chicago, Ill) scanner. The acquired spatial resolution was 1.5 × 1.5 × 3.0 mm with the z-direction zero-interpolation filling factor of two resulting in 1.5-mm reconstructed slices. Of 35 patients, 31 were imaged with velocity encoding of 250 cm/sec, while four patients were imaged with velocity encoding of 350 cm/sec. All scans were assessed for image quality by a fellowship-trained cardiovascular radiologist (A.H.). If a study was degraded by patient (motion or metallic hardware) or technical (suboptimal gating or aliasing) factors, it was excluded.

Flow Measurements

Volumetric flow measurements were calculated after background-phase correction and delineation of vessel ROIs on the CardioDL 2.3 (Arterys, San Francisco, Calif). Measurements were made at 14 locations by a single reader (M.H.) blinded to vorticity measures. In the aAo, measurements were made at the beginning of the aAo (sinotubular junction, aAo_1), end of the aAo (takeoff of the brachiocephalic artery, aAo_5), and at three equispaced locations within the ascending aorta ($aAo_{2–4}$). Along the mid-descending aorta ($dAo_{1–3}$), three measurements were made centered and equally spaced halfway between the aortic isthmus and the level of the diaphragmatic aortic hiatus. Three measurements were made equally spaced in the main pulmonary artery ($mPA_{1–3}$) and in the superior vena cava ($SVC_{1–3}$) below the azygos vein.

Mean pulmonary flow measurements and the sum of the mean descending aorta and SVC (dAo + SVC) flows were used as non-aortic measures of cardiac output, which have previously been shown to have high correlation to aortic measurements (16).

Visualization of Vorticity

A segmentation-free approach was developed to visualize regions of vorticity using the λ_2 method (10). Specifically, for each time point, we independently calculated the velocity gradient tensor and then performed eigenvalue decomposition on $S^2 + \Omega^2$. Pixels with negative λ_2 were multiplied by −1 to become positive and then transformed via a logistic function ($L = 1$, $k = 1 \times 10^{-6}$, $x_o =$

Table 1: Patient Demographics

Demographic	Value (n = 35)
Age (y)	58.6 ± 14.4 (28–87)
No. of women*	12 (34)
BMI (kg/m^2)	27.6 ± 4.6 (17–36)
Heart rate (beats/min)	61 ± 13 (44–96)
No. of ascending aortic aneurysm*	18 (51)
No. of bicuspid aortic valve*	10 (29)

Note.—Values are means ± standard deviations. Ranges are shown in parentheses, unless otherwise indicated. BMI = body mass index.
* Data in parentheses are percentages.

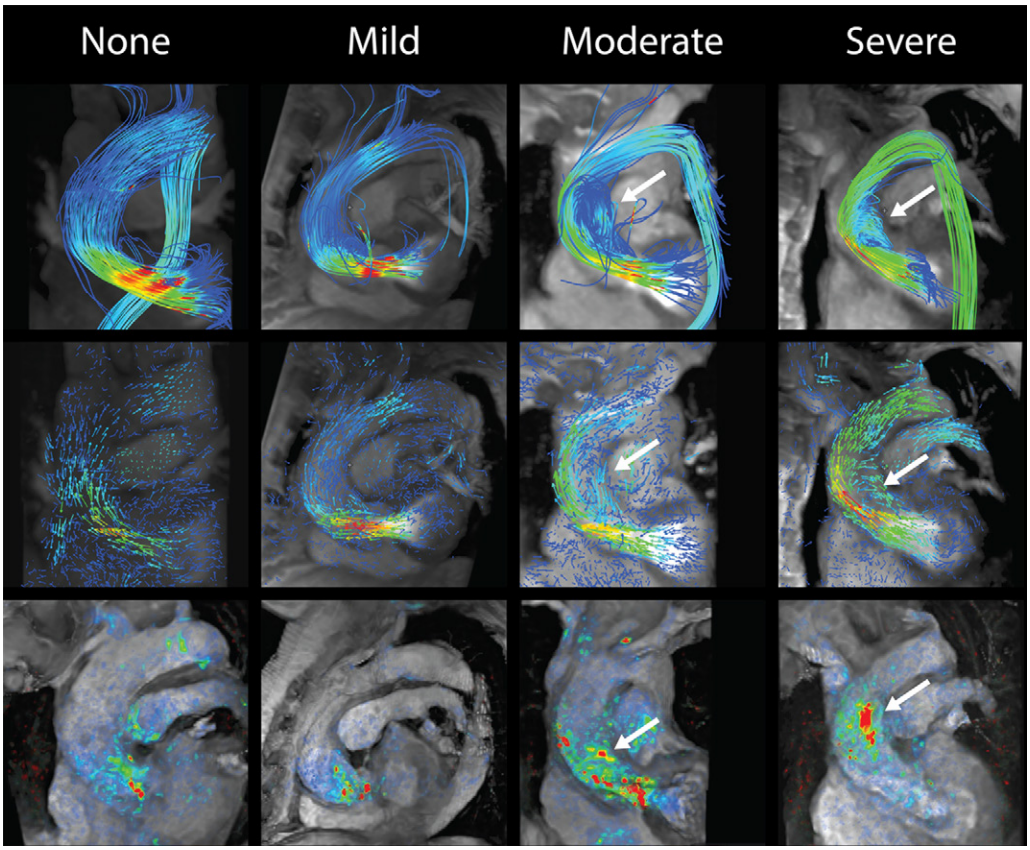

Figure 1: MR images with overlays of streamlines (top), vector fields (middle), and proposed vortex rendering (bottom) at peak systole in cases of none, mild, moderate, and severe vorticity. All cases except for moderate vorticity had aneurysmal ascending aortas (aAos). Flow patterns in the aAo span the spectrum from predominantly laminar to highly vortical. Specifically, vortical flow in the moderate and severe cases (indicated by white arrows) corresponds to regions of high vortical rendering above the level of the aortic valve.

3×10^6) to compress the dynamic range. Values were then multiplied with the magnitude image to mask low-signal (eg, air) regions and subsequently visualized on Arterys software. Vorticity in the aAo was visually scored as none (score of 0), mild (score of 1), moderate (score of 2), or severe (score of 3) by a single reader (F.C.) blinded to measurements of cardiac output. The reader evaluated the entire cardiac cycle and identified the frame with peak vorticity for scoring. Images representative of streamlines, vector fields, and vorticity at peak systole for each score are shown in Figure 1. Patients with moderate or severe vorticity were further analyzed to assess whether the vortical region was only in the proximal portion or whether it extended into the distal portions of the aAo.

Volumetric Assessment of Vorticity

To measure the vorticity core volume at each cardiac phase and observe the change over the cardiac cycle, the vorticity renderings were segmented using ITK-SNAP (Philadelphia, Pa) with a fixed binary threshold after logistic transformation (values > 5) (17).

Correlation between Visual and Quantitative Assessment of Vorticity

To evaluate whether the visual assessment of vorticity—which can be easily performed before flow quantification—correlates with subsequent segmentation of vorticity core pixels, we compared the visual vortex classification (none, mild, moderate, or severe) to maximum vortical volume (in milliliters) and the temporal integral of the vortical core (in milliliters second) from the entire cardiac cycle.

Correlation between Visual Classification and Differences in Measured Flow

We compared the presence of aneurysms, presence of a bicuspid aortic valve, the maximum aortic diameter, cardiac output measured at different locations, and standard deviation of cardiac output between patients with no or mild vorticity and those with moderate or severe.

Statistical Analysis

Statistical analysis was performed with Excel (Microsoft, Redmond, Wash). For paired data, such as parallel measurements in the same patient, paired two-sided t tests with a type I error threshold (α) of .05 for statistical significance were performed. For comparison of unpaired data, such as variance in measurements between low (none or mild) and high (moderate or severe) vorticity, F tests were performed with a type I error threshold (α) of .05 for statistical significance. Mean ± standard deviation values are reported for continuous variables.

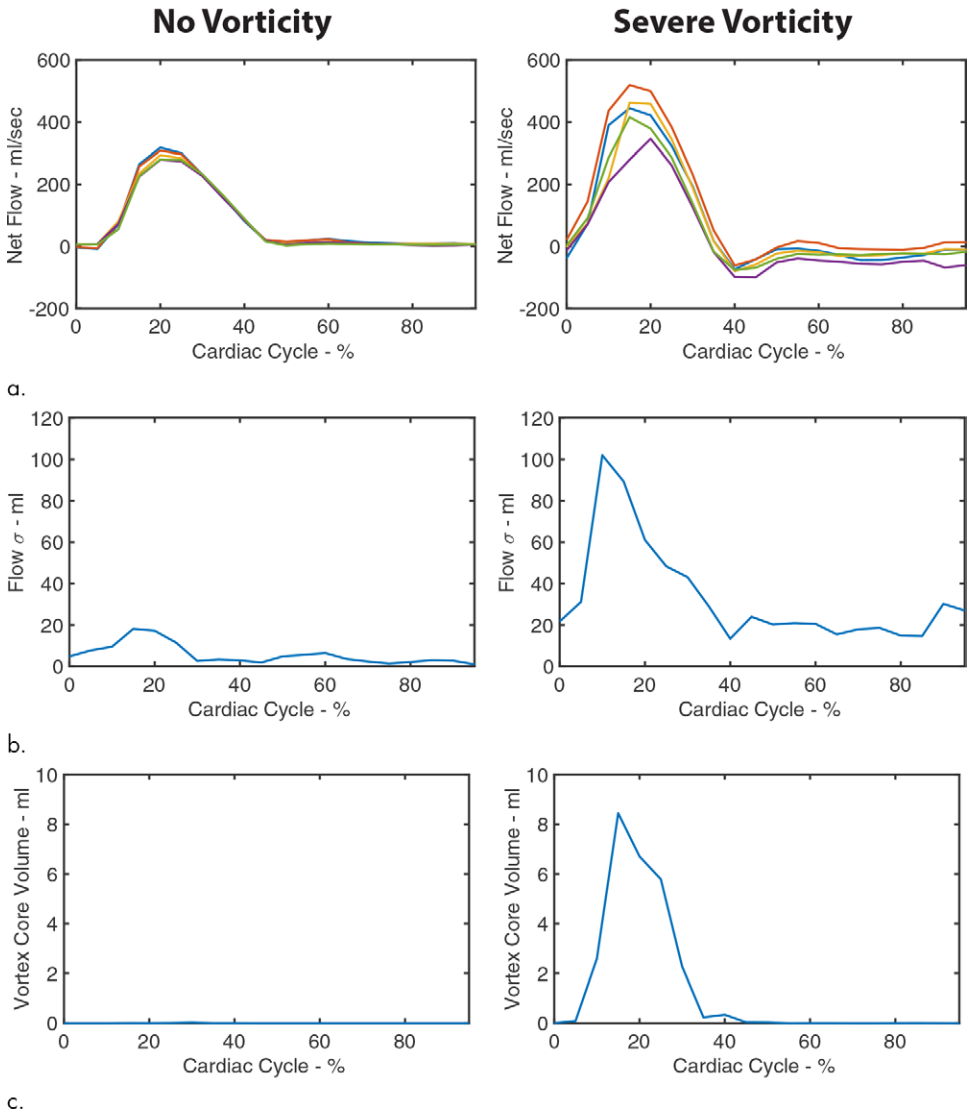

Figure 2: Graphs show relationship between ascending aortic (aAo) flow measurements, error, and vortex core volume as a function of the phase of the cardiac cycle for two exemplar patients (left: no vorticity, right: severe vorticity). **(a)** Flow measurements at five locations along the aAo. **(b)** Standard deviation of measured flow. **(c)** Volume of the vortex core as a function of cardiac phase. Flow measurement error temporally correlates with vortex core volume.

Results

MR Angiography and Flow Analysis

All 35 patients met the inclusion criteria, and no studies were excluded owing to technical factors. The average aortic diameter was 4.0 cm ± 0.6 ranging from 2.5 to 5.2 cm. Indexed to body surface area, the diameter was 2.1 cm/m^2 ± 0.4 ranging from 1.25 to 2.83 cm/m^2. In total, 18 out of 35 participants (51%) had aneurysmal aAos with a maximum diameter measurement of greater than 4.0 cm. In patients with aneurysmal aAos, the average aortic diameter was 4.5 cm ± 0.3 (indexed: 2.2 cm/m^2 ± 0.3), while patients without aneurysmal aAos had an average diameter of 3.5 cm ± 0.5 (indexed: 1.9 cm/m^2 ± 0.4). In total, 10 of the 35 patients had bicuspid aortic valves according to echocardiography reports and/or morphology of the aortic valve flow jet by 4D flow. Other pertinent patient demographic information is shown in Table 1.

Classification and Quantification of Vorticity Core Volume

Figure 2 shows flow measured at five positions along the aAo, the standard deviation of these flows, and the vortical core volume measured across the cardiac cycle for two patients. It illustrates high correlation between visual assessment of vorticity and flow inconsistency in the aAo. The 35 patients were visually classified as having no vorticity (n = 9), mild (n = 8), moderate (n = 11), or severe (n = 7). Agreement between visual classification of vorticity and vorticity volume is shown in Figure 3. Patients with more severe vorticity upon visualization had significantly higher maximum vorticity volume (3.6 mL ± 3.6 vs 0.5 mL ± 0.6; P < .001) and higher temporal integral of vortical core volume across the cardiac cycle (12.2 mL sec ± 11.3 vs 1.4 mL sec ± 1.8; P < .001). Of the 18 patients with moderate or severe vorticity, 10 had vortical visualizations that extended into the distal portion of the aAo.

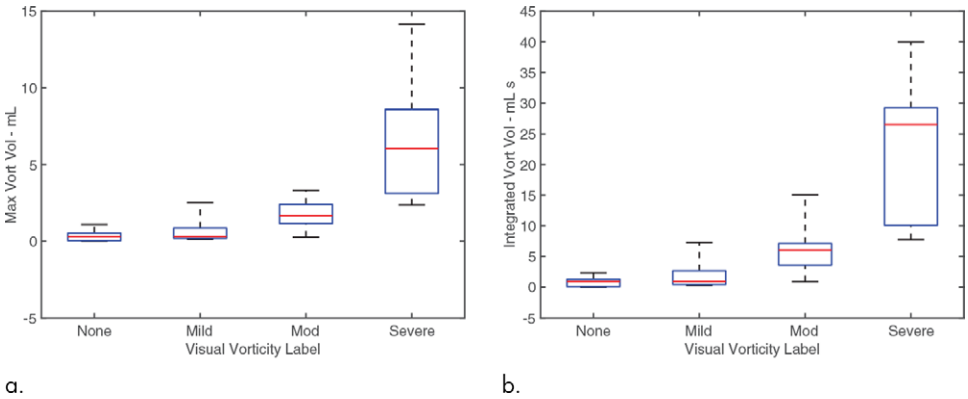

a. b.

Figure 3: Box plots show relationship between visual scoring of vorticity (n = 9 for none, n = 8 for mild, n = 11 for moderate, and n = 7 for severe) with **(a)** maximum vortex core volume and **(b)** temporal integral of vortex core volume. Red line indicates the mean.

Table 2: Differences in Aortic Caliber, Bicuspid Valve, and Cardiac Index Measurement among Patients with Low (None or Mild) or High (Moderate or Severe) Vorticity

Parameter	None or Mild Vorticity (n = 17)	Moderate or Severe Vorticity (n = 18)	P Value
No. of patients with presence of aneurysm	8	10	NA
No. of patients with presence of bicuspid valve	1	9	NA
Maximum ascending aorta diameter/BSA (mm)	2.01 ± 0.47	2.08 ± 0.26	.27
CO_{aAo} (L/min)	4.82 ± 1.37	5.73 ± 1.99	.06
CO_{PA} (L/min)	4.83 ± 1.36	6.13 ± 2.01	.02
$CO_{dAo+SVC}$ (L/min)	4.91 ± 1.35	6.05 ± 1.68	.02
SD of CO_{aAo} (L/min)*	0.44 ± 0.26	0.73 ± 0.55	<.01*
SD of CO_{mPA} (L/min)*	0.13 ± 0.09	0.17 ± 0.10	.86*
SD of $CO_{dAo+SVC}$ (L/min)*	0.12 ± 0.08	0.15 ± 0.09	.64*

Note.—Values are means ± standard deviations, unless otherwise specified. Patients with high vorticity showed greater standard deviation in cardiac index measurements in the ascending aorta (aAo) than patients with low vorticity. BSA = body surface area, CO = cardiac output, dAo = descending aorta, mPA = main pulmonary artery, NA = not applicable, PA = pulmonary artery, SD = standard deviation, SVC = superior vena cava.
* Indicates an F test was performed on variance values.

Correlation between Visual Classification and Differences in Measured Flow

Patients with moderate or severe vorticity (n = 18) were compared with patients with none or mild vorticity (n = 17). The impact of visual vortical classification on aneurysm prevalence, prevalence of bicuspid valve, maximum ascending aortic diameter, flow measures at different locations, and standard deviation of flow measured at different locations is shown in Table 2. In total, 10 (55%) of the 18 patients with moderate or severe vorticity had aneurysms compared with only eight (45%) of 17 patients with none or mild vorticity. Aneurysms were associated with an insignificant (P = .27) increase in maximum aortic diameters. Nine of 10 patients with bicuspid aortic valves were classified as having moderate or severe vorticity. Seven patients (out of 10 bicuspid valves and 18 aortic aneurysms) had both bicuspid valves and aortic aneurysms.

Table 2 shows cardiac output measured in the mPA and dAo + SVC were significantly higher in patients with moderate or severe vorticity (but the increase in aAo did not achieve statistical significance). The increase is likely due to differences in patient selection. The standard deviation of cardiac output observed in the aAo was significantly (P < .01) increased in patients with moderate or severe vorticity relative to none or mild while no significant differences were observed in the standard deviation of values measured in the mPA or dAo + SVC (P > .64).

Table 3 illustrates the mean, standard deviations, and range in cardiac output observed at the three measurement locations for all patients, as well as those with none or mild and moderate or severe vorticity. Across all patients, there were significant differences in cardiac output measured at the aAo and mPA (P = .02) and aAo and dAo + SVC CO (P = .04) but not between mPA and dAo + SVC CO (P = .49). However, these differences were not statistically significant in the vorticity subgroups (P > .28) likely owing to the small sample size. Across all patients and subgroups, the average standard deviation of cardiac output measured in the aAo (aortic valve and four ascending locations) was higher than the standard deviation observed in the three pulmonary arteries as well as the standard deviation in the three dAo + SVC measures. Across all groups and in the subgroups, the absolute and percentage standard deviations in the aAo were significantly (P < .006) higher than values measured from the pulmonary artery and dAo + SVC, and there was no significant difference (P > .27) between pulmonary artery and dAo + SVC values. Across all groups and in the subgroups, the range of values observed in the aAo was also significantly higher (P < .004) than values measured from the pulmonary artery and dAo + SVC, and there was no significant difference (P > .31) between pulmonary artery and dAo + SVC values.

In patients with moderate-to-severe vorticity (n = 18), the standard deviation of measured cardiac output was significantly (P = .02 on F test) higher in patients with vorticities that

spanned the proximal and distal portion of the aAo (0.44 L/min ± 0.35; n = 10) than in those with only proximal vortices (0.28 L/min ± 0.14; n = 8). The difference in flow between the proximal measure in the aAo (sinotubular junction) and the most distal aAo measure was significantly (P = .048) higher (0.94 L/min ± 0.78) in patients with vorticity throughout the aAo than those with only proximal vortices (0.49 L/min ± 0.35) (Fig 4).

Agreement between Measured Flow at Different Locations

As shown in Table 4, flow measured in the mPA and dAo + SVC demonstrated the lowest error and highest Pearson coefficient in the entire cohort. In cases where the aAo flow was compared with a different anatomic location, increased error was observed. The difference between mPA and dAo + SVC was significantly lower than the difference between mPA and aAo for patients with none or mild vorticity (P = .002) and patients with moderate or severe vorticity (P = .02). The difference in patients with moderate or severe vorticity did not achieve statistical significance (P > .16).

Discussion

In this study, we developed an automated approach for visualization of flow vorticity and demonstrated an association between regions with vortical flow and discrepancies in measured cardiac output within and between measurement locations. Specifically, we found that patients with the most severe vortical flow in the aAo also had the greatest inconsistency in flow measurement in these same regions. Meanwhile, regions with more laminar flow, such as the pulmonary artery, showed greater consistency in flow measurement. This suggests that problems with flow vorticity are earnestly tied and localized to the vessel they are observed in

Table 3: Cardiac Output Measurements at Multiple Locations

Patient Group and Vessel	μ_{CO} (L/min)	σ_{CO} (L/min)	σ_{CO} (%)	r_{CO} (L/min)	r_{CO} (%)
All					
aAo	5.3 ± 1.8	0.6 ± 0.5	13 ± 16	0.3–5.0	5–218
mPA	5.5 ± 1.8	0.2 ± 0.1	3 ± 2	0.1–0.6	1–16
dAo + SVC	5.5 ± 1.6	0.1 ± 0.1	3 ± 2	0.0–0.8	0–18
None or mild vorticity					
aAo	4.8 ± 1.4	0.4 ± 0.3	10 ± 7	0.3–2.6	5–56
mPA	4.8 ± 1.4	0.1 ± 0.1	3 ± 2	0.1–0.6	1–16
dAo + SVC	4.9 ± 1.4	0.1 ± 0.1	3 ± 2	0.0–0.6	0–17
Moderate or severe vorticity					
aAo	5.7 ± 2.0	0.7 ± 0.6	16 ± 22	0.3–5.0	6–218
mPA	6.1 ± 2.0	0.2 ± 0.1	3 ± 2	0.1–0.6	1–14
dAo + SVC	6.1 ± 1.7	0.2 ± 0.1	3 ± 2	0.1–0.8	2–18

Note.—Mean μ, standard deviation σ, and range r (maximum to minimum value) in cardiac output (CO) measured at multiple locations in the ascending aorta (aAo) (n = 5), main pulmonary artery (mPA) (n = 3), and sum of the descending aorta (dAo) and superior vena cava (SVC) (n = 3). There was greater measurement error in the aAo than the other two locations with increased variation in patients with visualized vorticity.

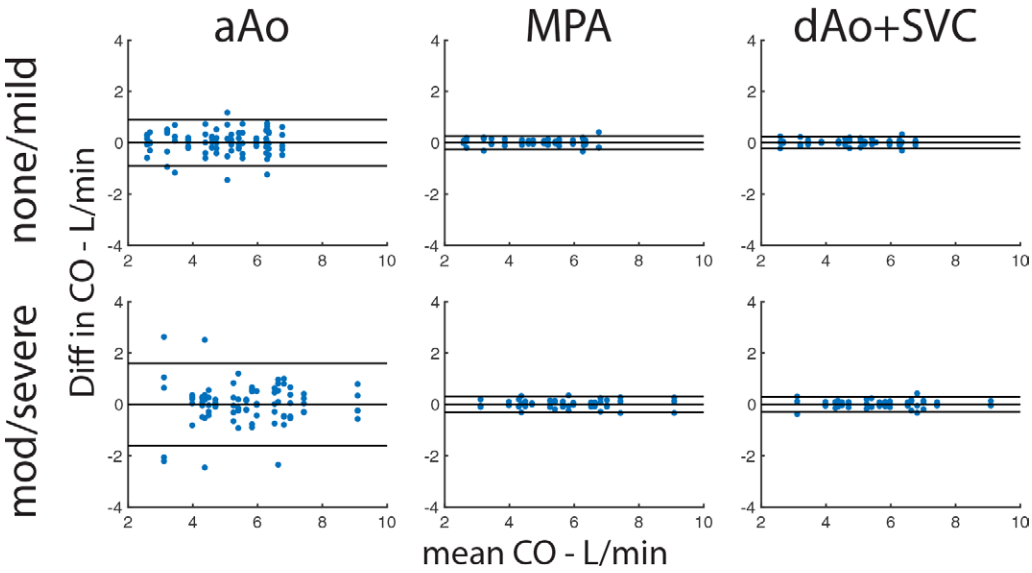

Figure 4: Difference in measured cardiac output (CO) for different measurement locations and visualized vorticity in ascending aorta (aAo). The mean CO was estimated as the average of the three locations (aAo, main pulmonary artery [MPA], and descending aorta [dAo] + superior vena cava [SVC]). The difference in CO is shown for each measurement at the location (n = 5 for aAo and n = 3 for mPA and dAo + SVC). The limits of agreement increased between patients with no or mild vorticity compared with those with moderate (mod) or severe from 20.0% to 36.9% in the aAo but remained unchanged in the mPA (6.0% to 5.4%) and the dAo + SVC (5.6% to 6.0%). Diff = difference.

Table 4: Statistical Assessment of Cardiac Output Measurements

Patient Group	Vessel of Interest	Reference	E_{CO}–L/min	ρ_{CO}
All	aAo	dAo + SVC	−0.21 ± 0.70	0.916
	aAo	mPA	−0.20 ± 0.60	0.945
	mPA	dAo + SVC	0.00 ± 0.54	0.959
None or mild vorticity	aAo	dAo + SVC	−0.09 ± 0.53	0.902
	aAo	mPA	−0.01 ± 0.35	0.910
	mPA	dAo + SVC	−0.08 ± 0.56	0.953
Moderate or severe vorticity	aAo	dAo + SVC	−0.32 ± 0.57	0.921
	aAo	mPA	−0.40 ± 0.36	0.960
	mPA	dAo + SVC	0.08 ± 0.55	0.957

Note.—Values are mean ± standard deviation. Error (E_{CO}) and Pearson (ρ_{CO}) coefficient of cardiac output measured at the ascending aorta (aAo), main pulmonary artery (mPA), and sum of descending aorta (dAo) and superior vena cava (SVC). Across the entire cohort of patients, cardiac output (CO) measurements at the mPA and sum of dAo and SVC were the two locations that were in greatest agreement.

and do not result in a complete corruption of the entire 4D flow acquisition. However, patients with mild disturbances in the aAo still had flow measurements consistent with surrogate locations, indicating that ascending aortic measurements are not always problematic.

In our study, we used flow measurements at a distance away from the aAo to highlight these as potential surrogate locations for measurement of cardiac output. The accuracy of this alternative may depend on the presence of laminar flow or confounding artifacts. It may not necessarily be true that these other locations are always better locations for blood flow measurement. For example, cardiac output measured in the pulmonary arteries may also be affected by aneurysmal dilatation, as can be seen in severe pulmonary hypertension (18) or long-standing shunts, which can perturb the laminar flow field strength assumption or affect measurements of blood flow volume. Thus, no single location is guaranteed to be optimal, and clinical judgment and experience is still required to weigh potentially discordant data from different locations. The location and size of the aortic vortices were rather varied in our patient population.

Although our results suggest the vortex location can be visualized to be either proximal or throughout the aAo, whether locations within the aAo, distant from a vortex, might still be useful to make accurate flow measurements remains unclear. The location, severity, and size of the vortex core may each have an effect. It is also uncertain how to optimally match the visualization of the vortex core to the inconsistencies in the flow vector field. For example, flow measurements in the distal aAo might still be accurate in the setting of a severe but small, proximal vortex. Exploring this further may require not only a much larger patient population but also a better understanding of how to optimally quantify and display the "size" of the vortex, which is not a well-defined problem from a fluid mechanics standpoint. Future studies may be required to solve this challenging fluid dynamics problem.

A few limitations should be considered. This was a retrospective study performed in 35 patients referred for evaluation of ascending aortic caliber. As a result, cine steady-state free precession was not available for volumetric comparison of cardiac output. However, the accuracy of 4D flow has been previously described (16,19–21). This is a population of patients for whom cardiac output measurements in the aAo are known in our practice to have greater error. We did not observe any vortical flow in the pulmonary arteries in our patient population, which allowed us to use this as a reference point in our study. However, it is unclear if vessels in other patient populations are affected by this phenomenon. We have observed a similar effect of high vorticity when quantifying mPA flow in patients with pulmonary hypertension, which is a population of patients that was not explored here. In other words, the relationship between flow vorticity and precise quantification of cardiac output may not be isolated to the aAo. Another limitation was that the impact of flow vorticity on flow measurements may not be equally severe on flow measurements obtained with different MRI platforms and pulse sequences, and there may be specific technical or pulse sequence factors that may mitigate this effect. However, to our knowledge, this relationship has not previously been reported. Finally, we did not directly correlate a quantitative measure of vortical core volume to the measurement error in the aAo but relied primarily on visual assessment. Future work may be required to determine optimal methods for defining vorticity core volume and thresholds where measurement may be too inaccurate to be clinically useful.

In conclusion, the presence of severe flow vortices correlated with greater variance in flow measurements in the aAo. As phase-contrast MRI serves as the clinical standard of reference for noninvasive quantification of blood flow, errors in blood flow quantification may affect patient care and decision making and ought to be mitigated. The automated visualization approach proposed here could be used as part of a clinical pipeline to help guide placement of ROIs for blood flow quantification. Flow vortex visualization may help determine if alternative sites should be considered for measurement of blood flow.

Author contributions: Guarantors of integrity of entire study, F.J.C., M.H., S.K., A.H.; study concepts/study design or data acquisition or data analysis/interpretation, all authors; manuscript drafting or manuscript revision for important intellectual content, all authors; approval of final version of submitted manuscript, all authors; agrees to ensure any questions related to the work are appropriately resolved, all authors; literature research, F.J.C., M.H., S.K., A.H.; clinical studies, M.H., E.M., A.H.; statistical analysis, F.J.C.; and manuscript editing, all authors

Disclosures of Conflicts of Interest: **F.J.C.** disclosed no relevant relationships. **M.H.** disclosed no relevant relationships. **E.M.** disclosed no relevant relationships. **S.K.** disclosed no relevant relationships. **A.H.** Activities related to the present article: disclosed no relevant relationships. Activities not related to the present article: consultant for Arterys; received grant funding through GE Healthcare; owns stock options of Arterys; has received travel or meeting accommodations through Arterys. Other relationships: disclosed no relevant relationships.

References

1. Nayak KS, Nielsen JF, Bernstein MA, et al. Cardiovascular magnetic resonance phase contrast imaging. J Cardiovasc Magn Reson 2015;17:71.
2. Hundley WG, Li HF, Hillis LD, et al. Quantitation of cardiac output with velocity-encoded, phase-difference magnetic resonance imaging. Am J Cardiol 1995;75(17):1250–1255.
3. Hsiao A, Alley MT, Massaband P, Herfkens RJ, Chan FP, Vasanawala SS. Improved cardiovascular flow quantification with time-resolved volumetric phase-contrast MRI. Pediatr Radiol 2011;41(6):711–720.
4. Vasanawala SS, Hanneman K, Alley MT, Hsiao A. Congenital heart disease assessment with 4D flow MRI. J Magn Reson Imaging 2015;42(4):870–886.
5. Markl M, Frydrychowicz A, Kozerke S, Hope M, Wieben O. 4D flow MRI. J Magn Reson Imaging 2012;36(5):1015–1036.
6. O'Brien KR, Cowan BR, Jain M, Stewart RAH, Kerr AJ, Young AA. MRI phase contrast velocity and flow errors in turbulent stenotic jets. J Magn Reson Imaging 2008;28(1):210–218.
7. Dyverfeldt P, Bissell M, Barker AJ, et al. 4D flow cardiovascular magnetic resonance consensus statement. J Cardiovasc Magn Reson 2015;17(1):72.
8. Epps B. Review of vortex identification methods. 55th AIAA Aerospace Sciences Meeting, Grapevine, Texas, January 9–13, 2017. Reston, Va: American Institute of Aeronautics and Astronautics, 2017; 1–22.
9. Köhler B, Born S, van Pelt RFP, Hennemuth A, Preim U, Preim B. A survey of cardiac 4D PC-MRI data processing. Comput Graph Forum 2017;36(6):5–35.
10. ElBaz MSM, Lelieveldt BPF, Westenberg JJM, van der Geest RJ. Automatic extraction of the 3D left ventricular diastolic transmitral vortex ring from 3D whole-heart phase contrast MRI using Laplace-Beltrami signatures. In: Camara O, Mansi T, Pop M, Rhode K, Sermesant M, Young A, eds. Statistical Atlases and Computational Models of the Heart. Imaging and Modelling Challenges. STACOM 2013. Lecture Notes in Computer Science, vol 8330. Berlin, Germany: Springer, 2014; 204–211.
11. Stalder AF, Frydrychowicz A, Harloff A, et al. Vortex core detection and visualization using 4D flow-sensitive MRI [abstr]. In: Proceedings of the Eighteenth Meeting of the International Society for Magnetic Resonance in Medicine. Berkeley, Calif: International Society for Magnetic Resonance in Medicine, 2010; 3708.
12. Elbaz MS, Calkoen EE, Westenberg JJ, Lelieveldt BP, Roest AA, van der Geest RJ. Vortex flow during early and late left ventricular filling in normal subjects: quantitative characterization using retrospectively-gated 4D flow cardiovascular magnetic resonance and three-dimensional vortex core analysis. J Cardiovasc Magn Reson 2014;16(1):78.
13. Garcia J, Barker AJ, Collins JD, Carr JC, Markl M. Volumetric quantification of absolute local normalized helicity in patients with bicuspid aortic valve and aortic dilatation. Magn Reson Med 2017;78(2):689–701.
14. Masutani EM, Contijoch F, Kyubwa E, et al. Volumetric segmentation-free method for rapid visualization of vascular wall shear stress using 4D flow MRI. Magn Reson Med 2018;80(2):748–755.
15. Cheng JY, Hanneman K, Zhang T, et al. Comprehensive motion-compensated highly accelerated 4D flow MRI with ferumoxytol enhancement for pediatric congenital heart disease. J Magn Reson Imaging 2016;43(6):1355–1368.
16. Chelu RG, Horowitz M, Sucha D, et al. Evaluation of atrial septal defects with 4D flow MRI—multilevel and inter-reader reproducibility for quantification of shunt severity. MAGMA 2019;32(2):269–279.
17. Yushkevich PA, Piven J, Hazlett HC, et al. User-guided 3D active contour segmentation of anatomical structures: significantly improved efficiency and reliability. Neuroimage 2006;31(3):1116–1128.
18. Han QJ, Contijoch F, Forfia PR, Han Y. Four-dimensional flow magnetic resonance imaging visualizes drastic changes in the blood flow in a patient with chronic thromboembolic pulmonary hypertension after pulmonary thromboendarterectomy. Eur Heart J 2016;37(36):2802.
19. Feneis JF, Kyubwa E, Atianzar K, et al. 4D flow MRI quantification of mitral and tricuspid regurgitation: reproducibility and consistency relative to conventional MRI. J Magn Reson Imaging 2018;48(4):1147–1158.
20. Hsiao A, Tariq U, Alley MT, Lustig M, Vasanawala SS. Inlet and outlet valve flow and regurgitant volume may be directly and reliably quantified with accelerated, volumetric phase-contrast MRI. J Magn Reson Imaging 2015;41(2):376–385.
21. Hsiao A, Lustig M, Alley MT, et al. Rapid pediatric cardiac assessment of flow and ventricular volume with compressed sensing parallel imaging volumetric cine phase-contrast MRI. AJR Am J Roentgenol 2012;198(3):W250–W259.